Vol. 43 — N° 3 09 19 p. 453–473

GEOSTANDARDS and GEOANALYTICAL RESEARCH

New Olivine Reference Material for *In Situ* Microanalysis

Valentina G. **Batanova** (1, 2)*, Jay M. **Thompson** (3), Leonid V. **Danyushevsky** (3), Maxim V. **Portnyagin** (2, 4), Dieter **Garbe-Schönberg** (5), Erik **Hauri**† (6), Jun-Ichi **Kimura** (7), Qing **Chang** (7), Ryoko **Senda** (7, 8), Karsten **Goemann** (9), Catherine **Chauvel** (1, 10), Sylvain **Campillo** (1), Dmitri A. **Ionov** (11) and Alexander V. **Sobolev** (1, 2)

(1) ISTerre, CNRS, IRD, IFSTTAR, University Grenoble Alpes, Grenoble, F-38000, France
(2) Vernadsky Institute of Geochemistry and Analytical Chemistry, Kosigin str 19, Moscow, 117991, Russia
(3) CODES, University of Tasmania, Hobart, TAS 7001, Australia
(4) GEOMAR Helmholtz Centre for Ocean Research, Kiel, Germany
(5) Institute of Geosciences, Kiel University, Kiel, Germany
(6) Department of Terrestrial Magnetism, Carnegie Institution of Washington, 5241 Broad Branch Rd NW, Washington, DC, 20015, USA
(7) Japan Agency for Marine-Earth Science and Technology (JAMSTEC), Yokosuka, Japan
(8) Faculty of Social and Cultural Studies, Kyushu University, Fukuoka, Japan
(9) Central Science Laboratory, University of Tasmania, Hobart, TAS 7001, Australia
(10) Institut de Physique du Globe de Paris, University of Paris, CNRS, Paris, F-75005, France
(11) Geosciences Montpellier, University of Montpellier, Montpellier, 34095, France
* Corresponding author. e-mail: valentina.batanova@univ-grenoble-alpes.fr
†Deceased.

A new olivine reference material – MongOL Sh11-2 – for *in situ* analysis has been prepared from the central portion of a large (20 × 20 × 10 cm) mantle peridotite xenolith from a ~ 0.5 My old basaltic breccia at Shavaryn-Tsaram, Tariat region, central Mongolia. The xenolith is a fertile mantle lherzolite with minimal signs of alteration. Approximately 10 g of 0.5–2 mm gem quality olivine fragments were separated under binocular microscope and analysed by EPMA, LA-ICP-MS, SIMS and bulk analytical methods (ID-ICP-MS for Mg and Fe, XRF, ICP-MS) for major, minor and trace elements at six institutions world-wide. The results show that the olivine fragments are sufficiently homogeneous with respect to major (Mg, Fe, Si), minor and trace elements. Significant inhomogeneity was revealed only for phosphorus (homogeneity index of 12.4), whereas Li, Na, Al, Sc, Ti and Cr show minor inhomogeneity (homogeneity index of 1–2). The presence of some mineral and fluid-melt micro-inclusions may be responsible for the inconsistency in mass fractions obtained by *in situ* and bulk analytical methods for Al, Cu, Sr, Zr, Ga, Dy and Ho. Here we report reference and information values for twenty-seven major, minor and trace elements.

Keywords: olivine, reference material, electron probe microanalysis, LA-ICP-MS, secondary ion mass spectrometry.

Received 19 Sep 18 – Accepted 16 Mar 19

Olivine is the most abundant mineral in the upper mantle and many ultramafic rocks, and is a common mineral in basalts and as inclusions in diamond. Recent studies show that olivine is one of the main sources of petrological and geochemical information on mantle geodynamic and melting processes (e.g., Sobolev *et al.* 2005, 2007, De Hoog *et al.* 2010). Especially informative are the mass fractions of Ni, Mn, Ca, Al, Cr, Co, Ti, Zn, P and Na as well as less abundant elements such as Li, Sc, V, Cu and Y (Wan *et al.* 2008, De Hoog *et al.* 2010, Mallmann and O'Neill 2013, Coogan *et al.* 2014). The mass fraction of these elements varies by several orders of magnitude, from a few ng g^{-1} to several thousand μg g^{-1}. Electron probe microanalysis (EPMA), laser ablation-inductively coupled plasma-mass spectrometry (LA-ICP-MS) and secondary ion mass spectrometry (SIMS), techniques used commonly to determine olivine compositions suffer – some (EPMA) to a lesser and others (LA-ICP-MS, Sylvester 2008) to a greater degree – from so-called 'matrix effects'. The objectives of using matrix-matched reference materials are (a) to serve as a primary calibrator for major elements to minimise matrix effects (for EPMA) and (b) to monitor the accuracy and precision of analysis. In this study, we characterise a new olivine reference material using several

doi: 10.1111/ggr.12266

analytical techniques to determine major, minor and trace elements.

Sample description and preparation

Compositionally, homogeneous olivine is common in xenoliths of mantle peridotites, which are unaffected by reaction with the transporting melt (e.g., Ionov 2007). After initial screening, mantle peridotite xenolith Sh11-2 from a basaltic breccia at Shavaryn-Tsaram (48.046 °N, 99.994 °W), Tariat region in central Mongolia (Press *et al.* 1986, Ionov 2007) was selected as a suitable source for the new olivine reference material. This sample, collected by D.A. Ionov and R.W. Carlson, is characterised by minimal alteration of pristine mantle minerals during and after its transport to the surface, sample homogeneity in terms of modal and chemical composition and microstructure, and relatively high contents of key minor and trace elements in olivine (e.g., Ca, Ni, Mn, Al, Ti, Cr). The size of the selected xenolith (20 × 20 × 10 cm) ensured that its inner part, which showed no evidence of contamination by the host magma, was large enough to provide a sufficient amount of large olivine grains (Figure 1a).

The xenoliths at Shavaryn-Tsaram are hosted by ~ 0.5 My old volcanic breccia and cinder deposits produced by an explosive sub-aerial eruption. The volcanic rocks and the xenoliths at Shavaryn-Tsaram show little evidence of post-eruption alteration, due to the young age, dry climate and absence of hydrothermal activity (Ionov and Hofmann 2007, Carlson and Ionov 2019).

The inner part of the xenolith (700 g) was crushed and sieved. Around 10 g of clean olivine fragments with grain sizes of 0.5–1 and 1–2 mm were hand-picked under a binocular microscope (Figure 1b). The fragments with a grain size of 1–2 mm were leached in 2 mol l^{-1} HCl for 2 h to remove surface contamination. Some olivine fragments were mounted in epoxy and polished for *in situ* microanalysis. A preliminary electron microprobe investigation of 240 polished fragments of olivine showed a fairly homogeneous composition for major (Fe, Mg, Si) and ten minor and trace elements (Na, Al, P, Ca, Ti, Cr, Mn, Co, Ni, Zn). Some micrometre-size mineral inclusions (one FeNi sulfide 60 μm in diameter, one Al spinel and several orthopyroxenes) were identified within analysed olivine fragments. Mounts with 120 fragments of polished olivine grains and four batches (0.5–1 g each) of clean olivine separates were distributed to six analytical laboratories for *in situ* and bulk analysis (Table 1).

Table 1.
List of participating laboratories, methods and analysts

LN	Institution, University	Analytical method	Analyst
1	ISTerre, University Grenoble Alpes, Grenoble, France	EPMA, Solution ICP-MS	V. Batanova, C. Chauvel, S. Campillo
2	CODES, University of Tasmania, Tasmania, Hobart Australia	Isotope dilution, Solution ICP-MS, LA-ICP-MS, XRF	J. Thompson, J. Thompson, L. Danyushevsky, J. Thompson
3	Japan Agency for Marine-earth science and technology (JAMSTEC), Yokosuka, Japan	Solution ICP-MS, LA-ICP-MS	Q. Chang, R. Senda, J-I. Kimura, Q. Chang
4	Christian Albrechts University of Kiel (CAU), Kiel, Germany	Solution ICP-MS, LA-ICP-MS	D. Garbe-Schönberg, M. Portnyagin
5	Carnegie Institution of Washington (CIW), Washington, USA	LA-ICP-MS, SIMS	E. Hauri
6	CSL University of Tasmania, Australia	EPMA	K. Goemann

LN, number of the Laboratory refers to the Institution, analytical methods and analyst(s).

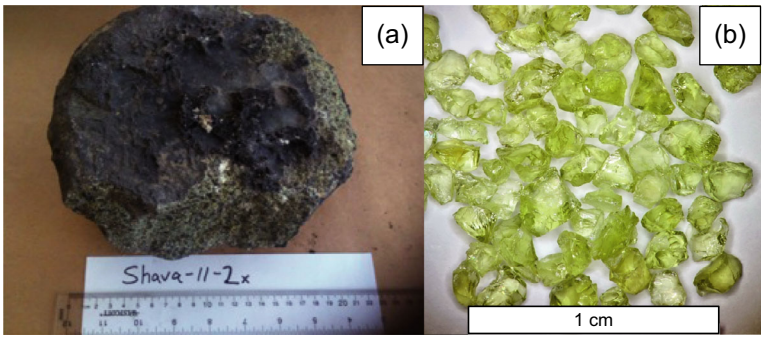

Figure 1. Photographs of (a) host xenolith of MongOL Sh11-2 olivine and (b) clean olivine fragments of grain size 1–2 mm. [Colour figure can be viewed at wileyonlinelibrary.com]

Analytical techniques

Bulk techniques

Clean olivine fractions (size 0.5–2 mm) were analysed using isotope dilution (ID) ICP-MS for Fe and Mg, solution ICP-MS and X-ray fluorescence (XRF) spectrometry.

Isotope dilution by ICP-MS: Analyses were performed at CODES Analytical Laboratories, University of Tasmania. Eight aliquots (combination of single grain and multiple grain aliquots) of whole olivine were picked and weighed on a high precision Satorius balance (d = 0.001 mg). Aliquots ranged in mass from ~ 4 to ~ 14 mg. Several international reference materials were also weighed for isotope dilution including BIR-1, BHVO-2 and DTS-2 (Jochum *et al.* 2005).

A ^{25}Mg and a ^{57}Fe isotope spike was added to each sample in a 7 ml beaker and precisely weighed on another balance (d = 0.01 mg). The ^{25}Mg spike was from *Inorganic Ventures* and is certified against NIST SRM 3131a for the concentration: 9.952 ± 0.058 μg ml^{-1} ^{25}Mg. The certified abundances of Mg isotopes (certified by Oak Ridge National Laboratories) are as follows: ^{24}Mg: 0.00963, ^{25}Mg: 0.98814, ^{26}Mg: 0.00223. The total certified Mg concentration is 10.068 ± 0.059 μg ml^{-1}.

The ^{57}Fe spike was also from *Inorganic Ventures* and is certified against NIST SRM 3126a for the concentration: 9.925 ± 0.062 μg ml^{-1} ^{57}Fe. The certified abundances of Fe isotopes (certified by Oak Ridge National Laboratories) are as follows: ^{54}Fe: 0.0022, ^{56}Fe: 0.0734, ^{57}Fe: 0.9244, ^{58}Fe: < 0.0005). The total certified Fe concentration is 10.721 ± 0.067 μg ml^{-1}.

Between 4–6 g of ^{25}Mg spike and 0.5–2 g of ^{57}Fe spike were added to each sample depending on mass of sample and estimated mass fractions of Mg and Fe. This was done to ensure similar sample to spike ratios in the analyses. Olivine was digested using a HF-HNO_3 mixture and was heated at 110 °C, and treated ultrasonically multiple times until the solution was visibly free of any olivine grain(s). The HF-HNO_3 mixture was then evaporated to dryness and refluxed several times in concentrated HNO_3 to ensure sample–spike equilibration and total digestion of the sample. Each sample was diluted into 2% HNO_3 to a final dilution of ~ 35000, giving roughly 8.5 μg g^{-1} Mg and 2.2 μg g^{-1} Fe in solution for the olivine samples.

To better constrain the concentrations of Mg and Fe in the spike solutions, reverse isotope dilution was performed using high purity Fe_2O_3 and MgO powders from Alfa Aesar. These were dried in an oven at 80 °C for several hours, then weighed into a Teflon digestion vessel and digested in Seastar HNO_3 (for the MgO) and Seastar HCl (for the Fe_2O_3), and gravimetrically diluted to a final volume of 250 ml. Next, an aliquot from each bottle was diluted into a 100 ml vial to give similar Fe and Mg concentrations to those expected from the olivine solutions and this was spiked with the ^{25}Mg and ^{57}Fe spike.

Samples were analysed using an Agilent 7700 ICP-MS with a collision cell and helium gas to remove polyatomic species. To avoid any potential complications with different detector modes (pulse vs. analogue counting), the isotopes of Fe and Mg were collected only in the analogue mode of ion detection, since count rates were > 1 Mcps, and to avoid any issues in changing ion detection modes on the isotope ratios. Data were collected in fifteen replicates with 200 sweeps of the quadrupole per replicate and took about 4.5 min per analysis. Solutions of pure Fe and Mg were measured throughout the analysis to correct for instrument mass bias (exponential law used) and monitor drift in the isotope ratios. No instrument drift was observed for either the Mg or Fe isotope ratios.

Isotope dilution results were calculated based on the ^{24}Mg/^{25}Mg and ^{56}Fe/^{57}Fe ratios, and concentrations calculated using the reverse isotope dilution results from the Mg and Fe spike solutions. Errors were propagated from the counting statistic errors on the analyses, error on the concentrations of Mg and Fe in the spikes (from the reverse isotope dilution) and error on the fractionation factor.

Minor and trace element measurement by ICP-MS: Measurements were performed at four laboratories: ISTerre, CODES Analytical Laboratories, JAMSTEC and CAU (Table 1). The details of the instruments, analytical conditions and reference materials' reproducibility are summarised in Table 2 and Table S1.

- ISTerre, University Grenoble Alpes. Olivine fragments with grain size 0.5–1 mm were leached in 2 mol l^{-1} HCl for ~ 2 h and powdered in an agate mill. Three separate 20–30 mg aliquots were dissolved in Parr bombs. Five measurements of each dissolution were made. The details of the analytical method are given in Chauvel *et al.* (2011). The ICP-MS signal was calibrated relative to the BHVO-2 contents compiled in Chauvel *et al.* (2011); individual element mass fractions were calculated using a BHVO-2 doped in Ni and a dilution of 5000 except for Al, which was calculated using a BHVO-2 not doped in Ni and with a dilution of 20000. Rock reference materials (BR24, BEN, UB-N and BIR-1a)

Table 2.
Summary of instruments, analytical conditions and reference materials used for solution ICP-MS analysis

Laboratory	L1 (ISTerre)	L2 (CODES)	L3 (JAMSTEC)	L4 (CAU)
ICP-MS instrument	Thermo X Series II	Agilent 7700x	Q-ICP-MS, Agilent, 7500ce	Agilent 7500cs
Plasma power	1400 W	1550 W	1.50 kW (27.12 MHz)	1500 W
Plasma Ar gas flow rate	13 l min^{-1}	15 l min^{-1}	15 l min^{-1}	14.8 l min^{-1}
Auxiliary Ar gas flow rate	0.79 l min^{-1}	0.8 l min^{-1}	0.89 l min^{-1}	0.89 l min^{-1}
Sample Ar gas flow rate	0.85 l min^{-1}	N/A	1.07 l min^{-1}	N/A
Carrier gas flow rate	0.85 l min^{-1}	0.83 l min^{-1}	0.76 l min^{-1}	0.87 l min^{-1}
Makeup gas flow rate	N/A	0.35 l min^{-1}	0.31 l min^{-1}	0.35 l min^{-1}
Sample cone	Normal (Ni) 1 mm orifice	Standard Pt cone	Normal (Pt) 1 mm orifice	Normal (Pt) 1.0 mm orifice
Skimmer cone	Normal (Ni) 0.8 mm orifice	Standard Pt cone	Normal (Pt) 0.8 mm orifice	Normal (Pt) 0.4 mm orifice
Nebuliser	Peltier cooled cyclonic spray chamber with a 400 µl PFA-ST nebuliser	Scott double pass	Peltier cooled Scott chamber with a 100 µl PFA nebuliser	Peltier cooled (2 °C) Scott chamber with a 100 µl PFA nebuliser
Typical sensitivity	75 Mcps/µg g^{-1} at ^{115}In in solution	4.1 Mcps/ng g^{-1}	0.1 Gcps/µg g^{-1} at ^{115}In in solution mode	0.2 Gcps/µg g^{-1} on ^{115}In
Oxide molecular	^{156}CeO/^{140}Ce 1.4%	^{156}CeO/^{140}Ce 1.9%	CeO/Ce < 1.5%	CeO/Ce < 1%
Detector mode	Pulse and analogue	Pulse and analogue	Dual mode	Pulse/analogue
Scan speed	1 s per scan	3.6 s	~ 1.5 s per scan	Variable
Acquisition time	90 s × 3	250 s	100 s × 5	408 s (136.1 s) per scan
Dilution factor	Calibration with BHVO-2 doped in Ni and a dilution of 5000 except for Al calibrated with BHVO-2, no dopping and a dilution of 20000	1000× for TE, 35000× for ID	2000× for trace elements and 20000× for major elements	800 (400× for digestion and 2× for analysis)
Reference materials	BHVO-2, BEN, BIR-1a, UB-N, BR24	Calibrated against custom multi-element reference solutions prepared from single element stock solutions, different manufacturers	Calibrated against multi-element reference solution from SPEX	Calibrated against custom multi-element reference solutions prepared from single element stock solutions, different manufacturers
Internal standard element	Be, Ge, In, Tm, Bi	Rh, In, Re	In, Bi	Be, In, Re
Control reference materials	% Relative bias	DTS-2, JP-1, BHVO-1, BIR-1	BIR-1, JP-1, JB-2	BIR-1, BHVO-2, JGb-1, % rel. bias
Monitored isotopes	^{7}Li, ^{23}Na, ^{27}Al, ^{31}P, ^{43}Ca, ^{45}Sc, ^{47}Ti, ^{51}V, ^{52}Cr, ^{55}Mn, ^{59}Co, ^{60}Ni, ^{63}Cu, ^{66}Zn, ^{71}Ga, ^{88}Sr, ^{89}Y, ^{90}Zr, ^{163}Dy, ^{165}Ho, ^{166}Er, ^{169}Tm, ^{172}Yb, ^{175}Lu	^{7}Li, ^{23}Na, ^{27}Al, ^{31}P, ^{43}Ca, ^{44}Ca, ^{45}Sc, ^{47}Ti, ^{49}Ti, ^{51}V, ^{52}Cr, ^{53}Cr, ^{55}Mn, ^{59}Co59, ^{60}Ni, ^{61}Ni, ^{62}Ni, ^{63}Cu, ^{66}Zn, ^{68}Zn, ^{71}Ga, ^{88}Sr, ^{89}Y, ^{90}Zr, ^{157}Gd, ^{159}Tb, ^{163}Dy, ^{165}Ho, ^{166}Er, ^{169}Tm, ^{172}Yb, ^{175}Lu	^{23}Na, ^{27}Al, ^{43}Ca, ^{45}Sc, ^{47}Ti, ^{51}V, ^{53}Cr, ^{55}Mn, ^{59}Co, ^{60}Ni, ^{63}Cu, ^{66}Zn, ^{88}Sr, ^{89}Y, ^{90}Zr, ^{91}Zr, ^{159}Tb, ^{163}Dy, ^{165}Ho, ^{166}Er, ^{169}Tm, ^{172}Yb, ^{175}Lu	^{7}Li, ^{23}Na, ^{27}Al, ^{31}P, ^{45}Sc, ^{49}Ti, ^{51}V, ^{52}Cr, ^{55}Mn, ^{59}Co, ^{60}Ni, ^{63}Cu, ^{66}Zn, ^{71}Ga, ^{88}Sr, ^{89}Y, ^{90}Zr, ^{163}Dy, ^{165}Ho, ^{166}Er, ^{169}Tm, ^{172}Yb, ^{175}Lu
Reference values	BR24 from Chauvel *et al.* (2011); BEN from Chauvel *et al.* (2011); BEN from Jochum *et al.* (2016); BIR-1 from Chauvel *et al.* (2011) for trace elements and Jochum *et al.* (2016) for major elements	Jochum *et al.* (2005) and multiple sources for some elements	JB-2 reference values from Makishima *et al.* (1999, 2002), Makishima and Nakamura (2006), others from Jochum *et al.* (2005)	Jochum *et al.* (2005) and multiple sources for some elements

were run as unknowns during the same measurement session. Results are provided in online supporting information Table S1. Values for BEN are from Chauvel *et al.* (2011) and Jochum *et al.* (2016); values for UB-N are from Chauvel *et al.* (2011).

- CODES Analytical Laboratories, University of Tasmania. Three aliquots (two of 0.5–1 mm size and one of 1–2 mm size) weighing ~ 40 mg each of olivine were digested and analysed five times each. To minimise contamination, all grains were inspected under an optical microscope and only the cleanest grains without identifiable inclusions were selected for digestion. The grains were then leached in 1 mol l^{-1} HCl for ~ 5 min to remove any surface contamination and then rinsed in DI H_2O several times. The samples were digested in HF-HNO_3 (2 and 1 ml, respectively) mixture on a hot plate (pre-cleaned Savillex Teflon) for 24 h at 110 °C.

Samples were then dried, and concentrated HNO_3 was added and evaporated to dryness several times. Samples were then reconstituted in 4 mol l^{-1} HNO_3 and diluted to give a 2% HNO_3 solution and a 1000× dilution. The solutions were analysed using an Agilent 7900x instrument, with He as the collision gas, in time-resolved data acquisition mode. The primary calibration was done using a mixture of pure-element solutions and was forced through the origin with ^{25}Mg and ^{115}In used for internal calibration. The following secondary reference materials were analysed in the measurement session: BIR-1, W-2, JP-1 and DTS-1 (Table S1). DTS-1 and JP-1 were digested using Parr bombs at 210 °C for 24 h to fully dissolve chromite, while other reference materials were digested using same procedure as for the olivine. Olivine data were corrected to rock reference materials BIR-1, W-2 and DTS-1 (the latter only for high abundance elements), while other reference materials were treated as unknowns. Since the analysis was done using a collision cell, no correction was made for ^{30}SiH interference on ^{31}P or for SiO interference on ^{45}Sc (Robinson *et al.* 1999, Yu *et al.* 2000, Norman *et al.* 2003) since it is expected that most of the Si was lost during the initial evaporation to dryness of the HF-HNO_3 for digestion. All reagents used were Seastar purity and Milli-Q DI water.

- Japan Agency for Marine-Earth Science and Technology (JAMSTEC). Olivine grains were inspected under optical microscopy and only the cleanest grains lacking identifiable inclusions were picked for digestion. The grains were then leached in 1 mol l^{-1} HCl for ~ 1 h to remove any surface contamination. One aliquot (0.5–1 mm size) of the olivine was digested and measured twice. Olivine grains were weighed in a 23 ml PFA Teflon vial. After adding concentrated $HClO_4$/HF (*v/v*: 25/75), the vial was capped tightly and placed on a hot plate at 130–140 °C for 3 days. $HClO_4$ instead of HNO_3 was used in this step, as it produces a more effective digestion of refractory minerals by improving the efficiency of the HF. The sample was then evaporated to incipient dryness to remove volatile SiF_4. Concentrated $HClO_4$ was added again, and the vial was closed and placed on a hot plate at 160 °C for 1 day, then opened to dry the sample at a gradually increasingly temperature of up to 190 °C, to drive out excess HF and to convert fluorides into chlorides. The residue was refluxed with 2 ml 6 mol l^{-1} HNO_3, moderately heated for 2 h and then dried down at a temperature of 120 °C to incipient dryness. The final sample residue was dissolved in 5 ml 2% HNO_3 and diluted to 2000 times for trace elements and 20000 times for major elements prior to analyses. An Agilent 7500ce in normal nebulisation mode was used for analysis. Element standard solutions (SPEX) were used to generate calibration curves. Isobaric overlap correction factors were determined using synthetic solutions. Reference materials JP-1, JB-2 and BIR-1 (Table S1) were analysed together, and the results exhibit reasonable fits with the reference values (Chang *et al.* 2003, Nakamura and Chang 2007). Since ^{45}Sc was within 9.6% RD for JP-1, no isobaric overlap correction was made.

- CAU Institute of Geosciences, Kiel. Two aliquots (0.5–1 and 1–2 mm grain size) of olivine grains were weighed in triplicate within 50 mg into 15 ml PFA (perfluoralkoxy) vials. After addition of mixed concentrated acids (HF-HNO_3-HCl) samples were digested on a hot plate overnight, and the resulting digest solutions were repeatedly evaporated to dryness and finally taken up in 20 ml of 3% *v/v* sub-boiled nitric acid. Prior to analysis, digest solutions were diluted twofold and spiked with 2.5 ng g^{-1} Be, In, Re for internal standardization. Subsequent analysis was done by ICP-MS using an Agilent 7500cs instrument in standard mode after calibration with freshly prepared multi-element standards (Garbe-Schönberg 1993). Results were blank-subtracted means of three runs. Analytical quality was monitored with procedural blanks during both digestion and sample preparation for analysis, and three replicate measurements of one olivine digest solution were used for assessing measurement precision. Basalt reference materials BIR-1 and BHVO-2 were used as secondary reference materials (Table S1) for checking the accuracy of the calibration and applying correction factors where necessary.

X-ray fluorescence spectrometry: XRF analyses were performed at CODES Analytical Laboratories, University of Tasmania on a PANalytical Axios Advanced WDS spectrometer using standard operating conditions. This technique was used to determine major and some minor elements. Two lithium borate fusion discs were made from the MongOL Sh11-2 olivine, consisting of 0.2 g of olivine, 0.3 g of high purity SiO_2, 4.5 g of 12/22 lithium borate flux (mixture of lithium metaborate and tetraborate) and 0.0606 g of $LiNO_3$. Each disc was analysed fifteen times, and greater variability between discs was seen than between repeated measurements with the RSD < 1% for all elements that were > 0.1% oxide in mass fraction. The olivine sample was diluted with the high purity SiO_2 due to the limited amount of the olivine sample. This had the advantage of bringing Mg and Ni values within the range of the instrument calibrations; however, minor elements such

as Ca, Al and Co were diluted to the point where they were close to the detection level. To assess the accuracy of the method, multiple (at least two) discs of several ultramafic reference materials (JP-1, PCC-1, DTS-1, DTS-2) were prepared with the same dilution of 0.2 g sample and 0.3 g SiO_2. A secondary correction was applied to the average of these ultramafic materials (from the primary calibration of the instrument) to account for: (a) the slight drift in the calibration for some elements with time and (b) any matrix effects of diluting the samples with the SiO_2.

In situ analytical techniques

Electron probe microanalysis: This technique was used at two laboratories to determine the mass fractions of major, minor and some trace elements, and to perform a major element homogeneity test of olivine fragments. Analyses were made on two different instruments (JEOL JXA-8230 and Cameca SX100) using different procedures for matrix correction, both laboratories used San Carlos olivine (USNM111312-44 (SCOL), Jarosewich *et al.* 1980) as a control reference sample (Table 3).

- ISTerre. Over 240 fragments of olivine with sizes from 0.5 to 2 mm were analysed in polished epoxy mounts using JEOL JXA-8230 electron probe using the trace element analytical method of Batanova *et al.* (2015) (Table 3). Accelerating voltage and probe current were 25 kV and 900 nA. The beam diameter was 2 μm. The ZAF correction procedure was applied to correct for matrix compositional effects. San Carlos olivine (USNM111312-44 (SCOL), Jarosewich *et al.* 1980) and ISTerre internal XEN olivine (Batanova *et al.* 2015, 2018) were run as unknowns three times after every batch of 30–40 measurements, in order to monitor potential instrumental drift and to estimate accuracy and precision. Additionally, ten grains were analysed using a 5 × 5 grid with a step from 100 to 300 μm.

- Central Science Laboratory, University of Tasmania. Analyses were performed on Cameca SX100. Operating conditions were as follows: accelerating voltage 20 kV; beam current 30 nA; beam diameter 5 μm. Calibration was performed using simple oxide reference materials (periclase for MgO, spectrosil for SiO_2, Smithsonian magnetite for Fe) and the 'Probe for EPMA' software (Probe Software, Inc.) with the Armstrong-Love-cott matrix correction method.

Laser ablation-ICP-MS: Minor and trace element analyses were performed at four LA-ICP-MS laboratories (Table 1) CODES Analytical Laboratories, JAMSTEC, CAU and CIW. An overview of the instruments, measurement conditions, reference materials and approaches to

Table 3.
Summary of instruments, analytical conditions and reference materials used for electron probe microanalysis

Laboratory	L1 (ISTerre)	L6 (CSL)
EPMA instrument	JEOL jxa-8230	Cameca SX100
Accelerating voltage	25 kV	20 kV
Beam current	900 nA	30 nA
Beam diameter	2 μm	5 μm
Matrix correction procedure/software	ZAF/JEOL	Armstrong/Love Scott, LINEMU MACs (Probe Software)
Measured X-ray line, spectrometer type and crystal/	Si Kα/EDS/SDD; Mg Kα/EDS/SDD; Fe Ka/EDS/SDD; Na Ka/WDS/TAP; Al Ka/WDS/TAP; P Ka/WDS/PETH;Ca Ka/WDS/PETH; TiKa/WDS/PETH; Cr Ka/WDS/LIFH; Mn Ka/WDS/LIFH; Co Ka/WDS/LIFL; Ni Ka/WDS/LIFH; Zn Ka/WDS/LIFL	Si Kα/WDS/TAP; Mg Kα/WDS/TAP; Fe Kα/WDS/LLiF; Al Kα/WDS/TAP; Ca Kα/WDS/LPET; Mn Kα/WDS/LPET; Ni Kα/WDS/LLiF
Peak/background total counting time (s)	Si, Mg, Fe 500 (live time); Na 160/160; Al 180/180; Ca 160/160; P180/180; Co160/160; Zn 180/180; Ti; 180/180; Ni 80/80; Mn 160/160; Cr 90/90	Si, Mg, Fe 30/10; Al, Ca, Mn 120/120; Ni 100/80
Primary reference material	Si, Mg, Fe olivine USNM111312-44 [a]; Na/Albite; Al/Al_2O_3; Ca/Wollastonite; P/Apatite Durango; Co/CoO; Zn/ZnS; Ti/TO_2; Ni/NiO; $Mn/MnSiO_3$; Cr/Cr_2O_3	Si/Spectrosil; Mg/Periclase; Fe/Magnetite USNM114887 [a]; Al/Corundum; Ca/Diopside [c]; Mn/Bustamite [c]; Ni/Nickel silicide [c]
Control reference sample	San Carlos olivine USNM111312-44 [a]; XEN-internal Lab olivine ref sample [b]	San Carlos olivine USNM111312-44 [a]

[a] Jarosewich *et al.* (1980), [b] Batanova *et al.* (2015), [c] Astimex Standards Ltd.

Table 4.
Summary of instruments, analytical conditions and reference materials used for LA-ICP-MS analysis

Laboratory	L2 (CODES)	L3 (JAMSTEC)	L4 (CAU)	L5 (CIW)
Laser ablation system	RESOlution S-155 equipped with a Coherent excimer laser	200/266 nm femtosecond laser ablation system (in-house) (OK Laboratory, OK-Fs2000K)	193 nm excimer laser ablation system GeoLas Pro (Coherent®)	Photon Machines ArF excimer
Laser source	CompexPro 193 nm laser	800 nm near infrared T-sappire one box regenerative amplifire, (Spectra Physics, Solstice)	Lambda Physics/Coherent CompexPro 102 (193 nm ArF)	ATLEX-SI 193 nm laser
Wave length (nm)	193	266 (frequency tripled by Spectra Physics, TP-1A THG)	193	193
Pulse width	~ 20 ns	< 170 fs for 266 nm	~ 20 ns	4 ns
Pulse energy	100 mJ	> 300 μJ at laser output, > 150 μJ at sample surface	145 mJ at 25 kV laser output	100 mJ
Fluence on sample (J cm^{-2})	10	~ 12	10	10
Beam diameter (μm)	70	90	90	50
Repetition rate (Hz)	10	10	10	10
Ablation mode	Fixed sample position	Rotation raster with initial circle diameter 15 μm, raster velocity ~ 10 μm s^{-1}	Single spot	Fixed sample position
Depth of crater	150 μm	~ 50 μm	n/a (300 pulses per spot)	~ 40 μm
Acquisition mode	Time resolved analysis with 30 s gas blank followed by 90 s acquisition	Time resolved analysis with 20 s gas blank, 60 s acquisition, and 80 s washout. Gas blanks: 15 s before ablation and after washout	Time resolved analysis with 20 s gas blank followed by 30 s acquisition	5 laser shots pre-ablation, 40 s washout, 25 s gas background, 25 s laser-on, 40 s washout
Carrier gas flow	He, 0.35 l min^{-1}	Ar, 1.0 l min^{-1}	He 1.00 l min^{-1}	Ar, 1.0 l min^{-1}
Additional gas flow	Ar, 1.05 l min^{-1}	He, 1.2 l min^{-1}	H_2 14 ml min^{-1}	He, 0.6 l min^{-1}
Ablation cell	S-155 two volume cell from Laurin Technic	In-house laminar flow cell	Zürich LDHCLAC Two-volume cell	
Smoothing device	Squid from Laurin Technic	In-house 17 cm^3 mixing chamber	None	
ICP-MS instrument	Agilent 7900	Thermo Fisher Scientific, ELEMENT XR. Reverse geometry high resolution sector field	Agilent 7500s quadrupole	Thermo iCapQ quadrupole
Plasma power	1.35 kW	1.35 kW (27.12 MHz)	1.5 kW	3.0 W
Guard electrode	N/A	Off (electrically disconnected)	Yes	N/A
Plasma gas flow	Ar, 14 l min^{-1}	Ar, 13 l min^{-1}	15 l min^{-1}	Ar, 14 l min^{-1}
Auxiliary gas flow	Ar, 0.8 l min^{-1}	Ar, 0.7 l min^{-1}	0.85 l min^{-1}	Ar, 0.6 l min^{-1}
Carrier gas flow	Ar, 1.05 l min^{-1}	Ar, 1.0 l min^{-1}	0.85 l min^{-1} Ar	Ar, 1.0 l min^{-1}
Sample cone	Pt cone	Normal (Ni)	Ni (1 mm)	Ni cone
Skimmer cone	Pt cone	Normal (Ni)	Ni (0.4 mm)	Ni cone
Mass resolution	0.7 amu	M/ΔM = 400 (low resolution)	0.75	M/ΔM = 200
Typical sensitivity	6300 cps/μg g^{-1} for ^{139}La when scanning at 3 μm s^{-1} with 40 μm beam at 10 Hz	20000 cps/μg g^{-1} ^{230}Th at 50 μm, 10 Hz, 8 J cm^{-2} (NIST SRM 612)	40000 cps/μg g^{-1} ^{139}La at 90 μm, 10 Hz, 13 J cm^{-2} (NIST SRM 612)	1.5 Mcps for ^{29}Si on San Carlos olivine
Oxide formation rate	ThO/Th < 0.2	ThO^+/Th^+ < 0.2%	ThO^+/Th^+ < 0.3%	ThO^+/Th^+ < 0.3%
Detector mode	Pulse/analogue	Triple or analogue (see text)	Pulse/analogue	Pulse/analogue
Scan speed	0.8 s	~ 2.6 s per scan	0.42 s	1.2 s
Dwell time (ms)	Specified in the text	5 or 10 ms/peak, 5 peaks/element	20	Variable by isotope
U/Th ratio (cps) on	1–1.05 on NIST SRM 612	1.05 on NIST SRM 612	1.07 on NIST SRM 612	1.05 on NIST SRM 612
Reference materials	NIST SRM 612, BCR-2G, GSD-1G	BHVO-2G	GOR-128G, GOR-132G, BM90/21G	MPI-DING, USGS, in-house CIW
Reference values	GeoReM preferred values	GeoReM preferred values	Jochum *et al.* (2016)	GeoReM preferred values
Internal standard element	Normalisation to 100%	Normalisation to 100%	Mg, Si	^{29}Si
Control reference materials	BCR-2G, GSD-1G	BCR-2G	GOR-128G, GOR-132G, BM90/21G	San Carlos 111312-42

Table 4 (continued).
Summary of instruments, analytical conditions and reference materials used for LA-ICP-MS analysis

Laboratory	L2 (CODES)	L3 (JAMSTEC)	L4 (CAU)	L5 (CIW)
Monitored isotopes	^{7}Li, ^{23}Na, ^{27}Al, ^{31}P, ^{43}Ca, ^{45}Sc, ^{49}Ti, ^{51}V, ^{53}Cr, ^{55}Mn, ^{59}Co, ^{62}Ni, ^{63}Cu, ^{66}Zn, ^{71}Ga, ^{88}Sr, ^{89}Y, ^{90}Zr, ^{163}Dy, ^{166}Er, ^{172}Yb	^{49}Ti, ^{27}Al, ^{55}Mn, ^{42}Ca, ^{23}Na, ^{31}P, ^{45}Sc, ^{51}V, ^{53}Cr, ^{59}Co, ^{60}Ni, ^{63}Cu, ^{66}Zn, ^{71}Ga, ^{88}Sr, ^{89}Y, ^{90}Zr, ^{163}Dy, ^{165}Ho, ^{166}Er, ^{169}Tm, ^{172}Yb, ^{175}Lu	^{7}Li, ^{23}Na, ^{27}Al, ^{31}P, ^{43}Ca, ^{45}Sc, ^{49}Ti, ^{51}V, ^{52}Cr, ^{55}Mn, ^{59}Co, ^{60}Ni, ^{63}Cu, ^{67}Zn, ^{71}Ga, ^{88}Sr, ^{89}Y, ^{90}Zr, ^{163}Dy, ^{166}Er, ^{172}Yb	^{7}Li, ^{23}Na, ^{27}Al, ^{31}P, ^{43}Ca, ^{45}Sc, ^{49}Ti, ^{51}V, ^{53}Cr, ^{55}Mn, ^{59}Co, ^{60}Ni, ^{63}Cu, ^{67}Zn, ^{71}Ga, ^{88}Sr, ^{89}Y, ^{90}Zr
Interference correction				
^{45}Sc (^{29}Si^{16}O)	Mass 45 measured on Spec-pure silica glass and extracted from the samples	No correction	^{29}Si^{16}O/^{29}Si = 0.035–0.065% (n = 14) was measured on synthetic nominally Sc free quartz and interpolated for other samples	Synthetic forsterite with of 0.07 μg g^{-1} Sc obtained by SIMS, used to determine SiO/Si ratio used for interference correction
^{67}Zn	No correction (^{66}Zn)	No correction (^{66}Zn)	Calculated as a function of Al_2O_3 based on RM measured	
^{31}P	Mass 31 measured on Spec-pure silica glass and interference subtracted from the samples			

quantification is presented in Table 4. Three laboratories used 193-nm Excimer lasers and one used 266-nm femtosecond laser operated at 10 Hz. The same 120 olivine fragments were analysed in each laboratory.

- CODES Analytical Laboratories. The laser microprobe was a RESOlution S-155 instrument equipped with a coherent 193 nm excimer laser of 20 ns pulse width. Ablation was performed at a fluence of 10 J cm^{-2}, with a 70 μm beam at 10 Hz. A 90 s ablation was preceded by a 30 s gas blank. A pre-ablation of five laser pulses was done prior to each analysis, and a 20 s washout between analyses was used. An Agilent 7900 ICP-MS was coupled to the laser and tuned for ThO/Th < 0.2 and U/Th of 1–1.05 using a line ablation of the NIST SRM 612 glass. The dwell times ranged from 5 to 20 ms depending on expected abundance of isotopes in olivine giving a total sweep time of 0.67 s. Gas flows were 0.35 l min^{-1} He through the ablation cell, which was mixed with Ar flowing at 1.05 l min^{-1} immediately after the ablation. The signal from the ablation cell was smoothed using the 'squid' signal-smoothing device (Müller *et al.* 2009). Calibration was performed on NIST SRM 612 for all elements except Fe and P, for which BCR-2G was used. ^{25}Mg was used as the internal standard element. Calibration reference materials were analysed twice after every ten analyses of the unknowns, using the same conditions as the unknowns. Data reduction was done using an in-house macro-based Excel workbook. Matrix effects were assessed and corrected by analysing BCR-2G and GSD-1G as secondary reference materials under the same conditions as the unknowns, after every ten analyses of the unknowns. All mass fractions for NIST SRM 612, BCR-2G and GSD-1G were taken from the GeoReM preferred values. Quantification was performed using conventional approaches (Longerich *et al.* 1996), with normalisation to 100% total of oxide components. A correction was applied for the ^{30}Si^{1}H and ^{29}Si^{16}O interference on ^{31}P and ^{45}Sc, respectively, by analysis of high purity Spectrosil silica glass analysed throughout measurement sessions. The correction was ~ 0.7% and ~ 2.2% for ^{31}P and ^{45}Sc, respectively. Total uncertainty of the reported mass fractions includes uncertainties of correction for instrumental drift during the session, matrix correction and the published values for secondary reference materials.

- JAMSTEC. A 266-nm wavelength, < 170 fs pulse width, 12 J cm^{-2} fluence laser pulse at 10 Hz was applied using an OK-Fs2000K laser ablation system (OK Lab, Tokyo, Japan) equipped with a Solstice one-box Ti: Sapphire 800-nm fs regenerative amplifier with TP-1A THG frequency tripling harmonic generator (Spectra-Physics, Santa Clara, CA, USA). The beam diameter was set at 90 μm and a circular raster protocol (15 μm radius, 10 μm s^{-1} raster velocity) was performed using a high precision sample translation stage to obtain a flat-bottomed crater of ~ 100 μm diameter and 50 μm depth after 60 s of ablation. An Element XR sector field ICP-MS (Thermo Fisher Scientific, Bremen, Germany) was modified by an additional high-efficiency interface vacuum pump and operated with N-sampler

H-skimmer cones and guard electrode (GE) disconnected to obtain low oxide ThO^+/Th^+ < 0.2% and U/Th = ~ 1.05 values. The laser aerosol carrier gas was He (at 1.2 l min^{-1}), which was mixed with Ar sample gas (at 1.0 l min^{-1}) in a mixing chamber (70 cm^3 inner volume) prior to the ICP torch. Analyses were performed in time-resolved mode with 20 s for gas blank, 60 s of LA signal acquisition and 80 s washout using gas blanks 15 s before ablation and after washout. Mass scan speed was ~ 2.6 s per cycle and acquisition was made in low-resolution mode (M/ΔM = 400) using a dual-mode ion counter for both major and trace elements. The reference material used was the USGS basaltic glass BHVO-2G for all the elements and was analysed before and after each five unknowns for calibration and drift correction. Laser ablation efficiency was corrected using total-100% normalisation using major oxides. The details of the interference corrections are in Table 4. Reference material glass BCR-2G was monitored for repeatability and reproducibility tests (Kimura and Chang 2012).

- CAU. Analyses were performed with an Agilent 7500s quadrupole mass-spectrometer coupled to a 193 nm excimer laser ablation system (GeoLas Pro; Coherent, Göttingen, Deutschland) using a 90 µm laser spot, a pulse frequency of 10 Hz and laser fluence of 10 J cm^{-2}. All analyses were performed in a large volume 'Zürich' ablation cell. The carrier gas was He (~ 1.05 l min^{-1}) with addition of H_2 (14 ml min^{-1}), which were mixed with Ar (0.85 l min^{-1}) before introduction into the mass spectrometer. Oxide production rate, estimated as $[ThO]^+/[Th]^+$, was < 0.3%. Analyses were performed in time-resolved mode and included 20 s background measurement followed by 20 s sample ablation and signal measurement. Dwell time was 20 ms for all elements. Scan speed was 0.68 s per cycle. All spectra were processed with GLITTER software. Mass fractions were quantified from the measured ion yields normalised to ^{25}Mg, ^{29}Si, ^{57}Fe and Mg, Si and Fe mass fractions from EPMA microprobe data. The data obtained using different reference elements were averaged. Analyses of MPI-DING reference glass KL2-G as well as one of glasses GOR-128G, GOR-132G and BM90/21G were performed every twenty olivine analyses and used for calibration and drift correction (Jochum *et al.* 2005, 2006). Isobaric interference of $^{29}Si^{16}O$ on ^{45}Sc was monitored and corrected by using data from Sc-free synthetic optical-grade quartz, which was measured together with reference glasses every twenty analyses. The details for the interference corrections are in Table 4. Typical Si oxide production rate on

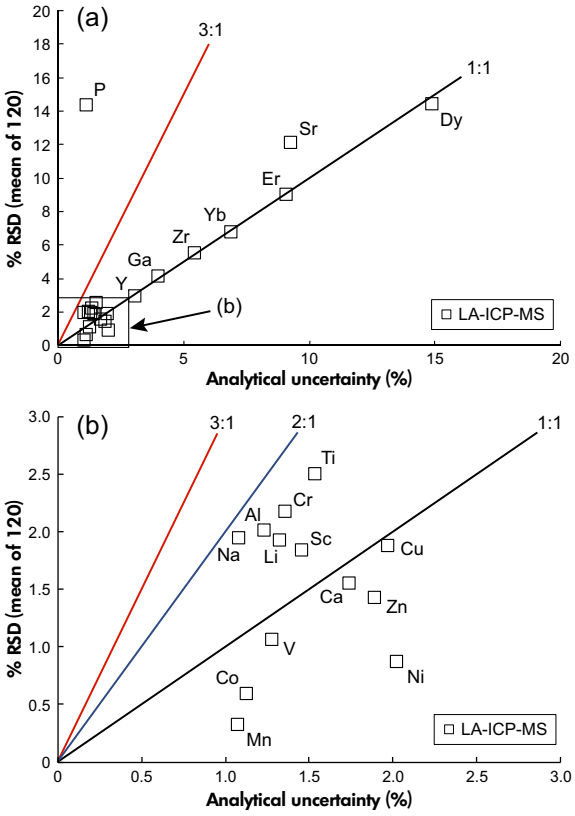

Figure 2. Assessment of homogeneity of olivine MongOL Sh11-2 on the basis of LA-ICP-MS analyses of 120 individual olivine fragments. Values of homogeneity index of 1 (black lines), 2 (blue line) and 3 (red lines) are shown. (a) The full range of values; note that P is the only element showing substantial heterogeneity. (b) Elements with % RSD values < 3%. See text for details.

mass 45 was 0.035–0.065% (n = 14). In the absence of Al-free reference samples, Zn mass fractions were quantified from the calibration using Al-bearing reference glasses corrected for the interference of ^{67}Zn with $^{27}Al^{40}Ar$. Matrix correction was applied for Al and Ca mass fractions based on analyses of an in-house (reference) pressed nanopowder of San Carlos olivine characterised previously by ICP-MS and EPMA.

- CIW. A Photon Machines 193 nm ArF excimer laser was coupled to a Thermo iCapQ quadrupole mass spectrometer. Analytical conditions were as follows: 7 mJ laser energy; 10 J cm^{-2} fluence; 50 µm diameter laser beam; 10 Hz repetition rate. Each analysis involved five laser shots pre-ablation followed by a wash-out of 40 s, 25 s of data acquisition of gas background (laser off)

Table 5.
Major element measurement results

Mass fraction (% *m/m*)	2*s*	2 RSD (%)	Method	LN
SiO_2				
40.79	0.27	0.66	EPMA	L 1
40.47	0.34	0.83	EPMA	L 6
40.96	0.21	0.52	XRF	L 2
MgO				
48.85	0.28	0.65	EPMA	L 1
48.68	0.42	0.86	EPMA	L 6
48.78	0.27	0.54	Isotope dilution	L 2
48.83	0.19	0.39	XRF	L 2
FeO				
10.16	0.07	0.68	EPMA	L 1
10.20	0.09	0.87	EPMA	L 6
10.17	0.09	0.87	Isotope dilution	L 2
10.16	0.04	0.42	XRF	L 2

and 25 s data acquisition during ablation (laser on). The details of interference corrections are in Table 4. Calibration reference materials included MPI-DING and USGS glasses (Jochum *et al.* 2005, 2006). The San Carlos olivine (USNM111312-44; Jarosewich *et al.* 1980) was used as a secondary reference material to correct for instrumental drift, and to perform secondary reference material corrections using the observed differences between the measured and accepted values.

Secondary ionisation mass spectrometry: Analyses were performed at CIW on a Cameca IMS 6F ion microprobe using energy filtering techniques (Shimizu and Hart 1982). The primary O^- ion beam had a current of 15 nA; the crater diameter was 30 μm. A field aperture was applied to mask surface contamination. A mass resolution power of 3500 was sufficient to resolve ^{29}SiO from ^{45}Sc, but not enough to resolve Ca dimers from ^{88}Sr, ^{89}Y and ^{90}Zr. The elements were determined using the ratio of their chosen isotope to ^{30}Si. Each measurement was preceded by 5 min of pre-sputtering. The masses measured were as follows: ^{7}Li, ^{9}Be, ^{11}B, ^{23}Na, ^{26}Mg, ^{27}Al, ^{31}P, ^{43}Ca, ^{45}Sc, ^{47}Ti, ^{51}V, ^{52}Cr, ^{55}Mn, ^{57}Fe, ^{59}Co, ^{60}Ni, ^{63}Cu, ^{88}Sr, ^{89}Y and ^{90}Zr. Interferences of Ca dimer (Ca^{2+}) on Sr, Y and Zr were not resolved. Calibration reference materials included MPI-DING and USGS glasses (Jochum *et al.* 2005, 2006). The San Carlos olivine (USNM111312-44; Jarosewich *et al.* 1980) was used as a secondary reference material to correct for instrumental drift.

Assessment of the homogeneity of olivine fragments

Chemical homogeneity can be defined as variation in element mass fraction, which does not exceed the measurement uncertainty of the analytical method (e.g., Boyd *et al.* 1967, Jarosewich *et al.* 1980, Potts *et al.* 1983, Jochum *et al.* 2000, Gilbert *et al.* 2013, Harries 2014). As suggested by the key international guide for the characterisation of reference materials (ISO Guide 35:2017), to examine homogeneity of olivine fragments in major elements (Si, Mg, Fe), the *F*-test for comparison of two population variances was applied. The three sets of EPMA measurements of MongOl Sh11-2 (each containing 36–95 separate fragments) were compared with repeated measurements (9–24) of single fragments of the San Carlos olivine USNM111312-44 (Jarosewich *et al.* 1980) that were run together with each set. The results of the *F*-test indicated that the standard deviations of all three populations of the different fragments of MongOl Sh11-2 are equal at the 95% confidence level to the standard deviations of the population of analyses of a single fragment of San Carlos olivine USNM111312-44 for all major elements (Table S2).

Additionally, in this study we used the homogeneity index (*H*) to assess homogeneity of minor and trace elements. *H* represents the ratio of the measurement uncertainty to the expected value of the total combined uncertainty (e.g., Boyd *et al.* 1967, Harries 2014, Pankhurst *et al.* 2017). A value of 1 for the index implies that the sample is homogeneous within the analytical uncertainty of individual measurements. A value > 3 for the index indicates significant chemical heterogeneity (e.g., Boyd *et al.* 1967, Jarosewich *et al.* 1980, Potts *et al.* 1983, Harries 2014, Pankhurst *et al.* 2017). The *H* value can be considered as a particular case of an *F*-test when the degree of freedom of each population approaches infinity (Harries 2014).

The assessment of homogeneity for minor and trace element was made using LA-ICP-MS data on 120 individual grains obtained at CODES Analytical Laboratories (Figure 2). The average within-run analytical uncertainty of individual measurements includes the uncertainties of the signal on the sample and reference materials, matrix correction and uncertainty related to the instrument drift during the session (e.g., Gilbert *et al.* 2013).

The observed variations in the uncertainty of individual analyses are due primarily to differences in element mass fractions (lower mass fractions result in higher signal noise) and isotopic abundance. Only phosphorus showed significant heterogeneity with a homogeneity index of 12.

Table 6.
Minor and trace element measurement results

MF (μg g^{-1})	2 RSD (%)	*U* (μg g^{-1})	Method	Lab	MF (μg g^{-1})	2 RSD (%)	*U* (μg g^{-1})	Method	Lab	MF (μg g^{-1})	2 RSD (%)	*U* (μg g^{-1})	Method	Lab	MF (μg g^{-1})	2 RSD (%)	*U* (μg g^{-1})	Method	Lab
Ti					**Na**					**Co**					**Ga**				
41	9.8	4.2	EPMA	L 1	115	13.7	17.8	EPMA	L 1	155	5.4	10.2	EPMA	L 1	0.105	13.9	0.014	LA-ICP-MS	L 3
30	9.3	1.7	LA-ICP-MS	L 3	137	7.7	5.8	LA-ICP-MS	L 3	147	15.0	5.8	XRF	L 2	0.097	8.2	0.003	LA-ICP-MS	L 2
38	5.0	1.3	LA-ICP-MS	L 2	119	3.9	4.2	LA-ICP-MS	L 2	136	5.5	6.2	LA-ICP-MS	L 3	0.098	10.8	0.004	LA-ICP-MS	L 4
33	10.0	1.3	LA-ICP-MS	L 4	111	4.4	6.0	LA-ICP-MS	L 5	151	1.2	3.1	LA-ICP-MS	L 2	0.137	3.2	0.003	SOL ICP-MS	L 2
38	6.4	1.2	LA-ICP-MS	L 5	158	42.0	8.6	SIMS	L 5	152	5.9	8.3	LA-ICP-MS	L 4	0.123	10.2	0.004	SOL ICP-MS	L 4
39	7.5	1.9	SIMS	L 5	134	2.7	1.1	SOL ICP-MS	L 2	145	2.5	4.4	LA-ICP-MS	L 5	**Sr**				
49	7.0	1.4	SOL ICP-MS	L 3	124	2.4	1.9	SOL ICP-MS	L 1	151	9.4	7.6	SIMS	L 5	0.008	122.0	0.0004	LA-ICP-MS	L 3
41	1.6	0.9	SOL ICP-MS	L 2	147	12.9	6.7	SOL ICP-MS	L 3	153	4.7	2.6	SOL ICP-MS	L 3	0.007	24.2	0.0003	LA-ICP-MS	L 2
45	5.7	2.0	SOL ICP-MS	L 1	**P**					142	2.7	4.5	SOL ICP-MS	L 2	0.007	51.5	0.0002	LA-ICP-MS	L 4
Al					59	24.0	5.7	EPMA	L 1	148	2.4	3.2	SOL ICP-MS	L 1	0.007	62.9	0.0005	LA-ICP-MS	L 5
236	5.3	9.0	EPMA	L 1	60	11.6	3.9	XRF	L 2	133	2.9	3.2	SOL ICP-MS	L 4	0.29	44.4	0.5000	SOL ICP-MS	L1
248	16.0	37.0	EPMA	L 6	75	17.6	5.2	LA-ICP-MS	L 3	**Ni**					0.10	26.8	0.0080	SOL ICP-MS	L2
239	24.0	10.0	XRF	L 2	63	28.7	1.9	LA-ICP-MS	L 2	2881	0.6	11.7	EPMA	L 1	0.20	69.4	0.0500	SOL ICP-MS	L3
205	8.4	2.0	LA-ICP-MS	L 3	58	18.4	3.5	LA-ICP-MS	L 4	2856	3.5	71.0	EPMA	L 6	0.20	129.6	0.074	SOL ICP-MS	L4
245	4.0	5.0	LA-ICP-MS	L 2	65	19.4	2.6	LA-ICP-MS	L 5	2758	1.0	42.0	XRF	L 2	**Y**				
243	9.1	28.0	LA-ICP-MS	L 4	89	26.8	4.7	SIMS	L 5	2403	5.9	146.0	LA-ICP-MS	L 3	0.073	15.4	0.006	LA-ICP-MS	L 3
222	4.2	9.0	LA-ICP-MS	L 5	84	2.8	7.7	SOL ICP-MS	L 2	2878	1.7	99.7	LA-ICP-MS	L 2	0.074	5.9	0.001	LA-ICP-MS	L 2
279	12.4	14.0	SIMS	L 5	**Sc**					2817	5.6	124.0	LA-ICP-MS	L 4	0.065	11.7	0.002	LA-ICP-MS	L 4
215	11.0	8.0	SOL ICP-MS	L 3	3.6	9.7	0.23	LA-ICP-MS	L 3	2805	2.8	84.6	LA-ICP-MS	L 5	0.076	19.7	0.003	LA-ICP-MS	L 5
310	1.3	4.0	SOL ICP-MS	L 2	3.3	3.7	0.10	LA-ICP-MS	L 2	2769	10.0	138.8	SIMS	L 5	0.082	15	0.004	SOL ICP-MS	L 3
283	4.7	8.0	SOL ICP-MS	L 1	3.5	10.7	0.11	LA-ICP-MS	L 4	2859	0.2	8.0	SOL ICP-MS	L 3	0.080	2.7	0.003	SOL ICP-MS	L 2

GEOSTANDARDS and GEOANALYTICAL RESEARCH

Table 6 (continued).
Minor and trace element measurement results

MF (µg g^{-1})	2 RSD (%)	*U* (µg g^{-1})	Method	Lab	MF (µg g^{-1})	2 RSD (%)	*U* (µg g^{-1})	Method	Lab	MF (µg g^{-1})	2 RSD (%)	*U* (µg g^{-1})	Method	Lab	MF (µg g^{-1})	2 RSD (%)	*U* (µg g^{-1})	Method	Lab
					2.8	4.2	0.20	LA-ICP-MS	L 5	2794	1.6	57.4	SOL ICP-MS	L 2	0.144	3.6	0.003	SOL ICP-MS	L 1
Mn					2.4	5.8	0.12	SIMS	L 5	2860	2.5	67.0	SOL ICP-MS	L 1	0.091	29.6	0.008	SOL ICP-MS	L 4
1132	0.7	7.7	EPMA	L 1	3.3	0.6	0.03	SOL ICP-MS	L 3	2339	3.0	51.0	SOL ICP-MS	L 4	**Zr**				
1113	2.8	29.0	EPMA	L 6	4.1	2.4	0.14	SOL ICP-MS	L 2	**Cu**					0.043	27.7	0.002	LA-ICP-MS	L 3
1106	2.2	33.1	XRF	L 2	3.2	1.6	0.09	SOL ICP-MS	L 1	1.1	8.2	0.10	LA-ICP-MS	L 3	0.043	11.0	0.001	LA-ICP-MS	L 2
1081	5.4	58.0	LA-ICP-MS	L 3	3.4	2.8	0.10	SOL ICP-MS	L 4	1.2	3.7	0.03	LA-ICP-MS	L 2	0.039	20.6	0.001	LA-ICP-MS	L 4
1107	0.6	44.3	LA-ICP-MS	L 2	**V**					1	6.2	0.07	LA-ICP-MS	L 4	0.050	34.1	0.005	LA-ICP-MS	L 5
1155	7.9	71.4	LA-ICP-MS	L 4	4.61	4.7	0.3	LA-ICP-MS	L 3	1.04	29.2	0.12	LA-ICP-MS	L 5	0.099	45.4	0.020	SOL ICP-MS	L 3
1217	2.2	37.0	LA-ICP-MS	L 5	5.24	2.1	0.2	LA-ICP-MS	L 2	1.23	12.4	0.06	SIMS	L 5	0.081	17.3	0.004	SOL ICP-MS	L 2
1139	8.2	57.0	SIMS	L 5	5.55	6.7	0.4	LA-ICP-MS	L 4	1.05	27.3	0.10	SOL ICP-MS	L 3	0.427	6.9	0.015	SOL ICP-MS	L 1
1127	2.3	21.0	SOL ICP-MS	L 3	5.47	3.4	0.2	LA-ICP-MS	L 5	0.92	1.7	0.01	SOL ICP-MS	L 2	0.148	73.0	0.031	SOL ICP-MS	L4
1140	1.8	8.6	SOL ICP-MS	L 2	5.26	7.2	0.3	SIMS	L 5	**Zn**					**Li**				
1090	3.0	15.3	SOL ICP-MS	L 1	5.89	2.5	0.1	SOL ICP-MS	L 2	60	17.7	13.1	EPMA	L 1	1.95	3.8	0.03	LA-ICP-MS	L 2
					6.09	5.1	0.2	SOL ICP-MS	L 1	57	34.0	4.0	XRF	L 2	1.91	18.2	0.16	LA-ICP-MS	L 4
Ca					6.05	5.4	0.14	SOL ICP-MS	L 4	56	5.7	3.3	LA-ICP-MS	L 3	2.34	13.9	0.17	LA-ICP-MS	L 5
687	1.4	6.0	EPMA	L 1	**Cr**					58	2.9	1.2	LA-ICP-MS	L 2	2.39	29.2	0.13	SIMS	L 5
688	3.8	19.0	EPMA	L 6	126	7.7	9.0	EPMA	L 1	57	5.4	3.0	LA-ICP-MS	L 4	2.15	9.9	0.10	SOL ICP-MS	L 2
688	12.0	9.5	XRF	L 2	99	22.0	6.1	XRF	L 2	54	4.5	1.6	LA-ICP-MS	L 5	2.11	2.4	0.08	SOL ICP-MS	L 1
525	9.2	5.3	LA-ICP-MS	L 3	115	6.8	5.0	LA-ICP-MS	L 3	54	1.4	1.3	SOL ICP-MS	L 2	2.50	5.0	0.05	SOL ICP-MS	L 4
718	3.1	11.4	LA-ICP-MS	L 2	122	4.3	7.7	LA-ICP-MS	L 2	54	1.7	3.2	SOL ICP-MS	L 1					

Table 6 (continued).
Minor and trace element measurement results

MF (µg g^{-1})	2 RSD (%)	U (µg g^{-1})	Method	Lab	MF (µg g^{-1})	2 RSD (%)	U (µg g^{-1})	Method	Lab	MF (µg g^{-1})	2 RSD (%)	U (µg g^{-1})	Method	Lab	MF (µg g^{-1})	2 RSD (%)	U (µg g^{-1})	Method	Lab
629	11.1	77.0	LA-ICP-MS	L 4	129	10.9	9.0	LA-ICP-MS	L 4	52	3.1	0.9	SOL ICP-MS	L 4					
594	22.5	26.4	LA-ICP-MS	L 5	125	3.9	4.0	LA-ICP-MS	L 5										
637	9.9	32.0	SIMS	L 5	126	8.7	6.3	SIMS	L 5										
576	13.8	28.0	SOL ICP-MS	L 3	132	7.2	3.4	SOL ICP-MS	L 3										
638	2.2	8.8	SOL ICP-MS	L 2	124	2.9	4.4	SOL ICP-MS	L 2										

MF, mass fraction; 2 RSD%, two relative standard deviations of individual analyses (dispersion of the data); *U*, overall uncertainty of analytical method provided by each laboratory.

Several elements showed minor inhomogeneity with homogeneity indices of < 2: Li (1.5), Na (1.8), Al (1.6), Sc (1.3), Ti (1.6), Cr (1.6) and Sr (1.3) (Figure 1b). All other elements were found to be homogeneous within the analytical uncertainty.

Measurement results and suggested reference values

A total of over 1020 *in situ* analyses were performed in this study on 120 olivine grains by EPMA, LA-ICP-MS and SIMS. Eight aliquots were analysed by ID-ICP-MS, nine aliquots were analysed by solution ICP-MS and two aliquots by XRF. Tables 5–7 list all analytical results provided by each laboratory, including analytical uncertainties expressed as two relative standard deviations in per cent (2 RSD), displaying the dispersion of the data (the measured reproducibility). Additionally, in Table 7 we show the overall analytical uncertainty (*U*) that includes instrumental repeatability, calibration errors and uncertainty of reference materials. Consistency of the data obtained in different laboratories by different analytical techniques is considered a measure of data quality. The preferred reference values are in Table 8, which shows statistical uncertainty: 2*s* – two standard deviation and 2SE – two standard deviation of the mean [sometimes incorrectly called 'standard error' (GUM 2008, Potts 2012), which corresponds to the 95% confidence level]. The latter is also expressed in relative % (Table 8).

Major elements (Si, Mg, Fe)

Measurement results for major elements (Si, Mg, Fe) are summarised in Table 5. For Fe and Mg, the isotope dilution analysis using ICP-MS is considered as the primary method with the highest metrological properties (Jochum *et al.* 2016). EPMA data obtained by both laboratories and XRF data are in good agreement with ID-ICP-MS and thus have been included in determination of reference values. The calculated reference values are in Table 8.

Minor and trace elements

To produce reference values, the data were treated with a filtering procedure proposed by the European Commission IRMM (Application Note 1 2010). This procedure considers the uncertainty of individual measurement results.

For each element, a 'global' average (C_{glob}) and standard deviation of the mean (U_{gl}) were first calculated for the values obtained by different techniques in different laboratories. We then compared this 'global' average with

Table 7.
Measurement results for high atomic number REE

MF (μg g^{-1})	Uncertainty 2 RSD (%)	Method	L N	MF (μg g^{-1})	Uncertainty 2 RSD (%)	Method	L N
Dy				**Tm**			
0.006	69.9	LA-ICP-MS	L 3	0.003	45.9	LA-ICP-MS	L 3
0.006	28.8	LA-ICP-MS	L 2	0.003	10.2	SOL ICP-MS	L 3
0.007	109.3	LA-ICP-MS	L 4	0.003	1.1	SOL ICP-MS	L 2
0.010	34.1	SOL ICP-MS	L 3	< 0.004	8.9	SOL ICP-MS	L 4
0.008	5.0	SOL ICP-MS	L 2	**Yb**			
0.010	7.7	SOL ICP-MS	L 1	0.028	29.3	LA-ICP-MS	L 3
< 0.02	35.6	SOL ICP-MS	L 4	0.030	13.5	LA-ICP-MS	L 2
Ho				0.028	52.1	LA-ICP-MS	L 4
0.002	54.5	LA-ICP-MS	L 3	0.031	6.4	SOL ICP-MS	L 3
0.004	21.8	SOL ICP-MS	L 3	0.028	5.9	SOL ICP-MS	L 2
0.003	4.4	SOL ICP-MS	L 2	0.030	5.3	SOL ICP-MS	L 1
0.003	10.0	SOL ICP-MS	L 1	0.032	7.3	SOL ICP-MS	L 4
< 0.0040	27.1	SOL ICP-MS	L 4	**Lu**			
Er				0.007	29.0	LA-ICP-MS	L 3
0.012	39.3	LA-ICP-MS	L 3	0.007	0.7	SOL ICP-MS	L 3
0.012	18.0	LA-ICP-MS	L 2	0.007	4.3	SOL ICP-MS	L 2
0.012	72.6	LA-ICP-MS	L 4	0.006	7.9	SOL ICP-MS	L 1
0.014	18.2	SOL ICP-MS	L 3	0.007	4.6	SOL ICP-MS	L 4
0.012	4.5	SOL ICP-MS	L 2				
0.014	13.2	SOL ICP-MS	L 1				
0.014	20.1	SOL ICP-MS	L 4				

MF, mass fraction.

the mean values obtained by different techniques in different laboratories (Figures 3–5). The absolute difference between the mean value and 'global average' was calculated as:

$$\Delta_m = |C - C_{glob}| \quad (1)$$

The uncertainty of Δ_m (U_Δ) was calculated from the uncertainty of the 'global average' and uncertainty of the measurement result U (Table 7):

$$U_\Delta = (2U^2 + 2U_{gl}^2)^{1/2} \quad (2)$$

A value is accepted if $\Delta_m \leq U\Delta$, if $\Delta_m > U\Delta$ the value is considered an outlier and is discarded (Figures 3–5). The preferred reference values were calculated as the mean of consistent values obtained by different methods in different laboratories (Table 8).

Na, Al, P, Ca, Ti, Cr, Mn, Co, Ni and Zn

For this group of ten elements with mass fraction levels greater than 10 μg g^{-1}, nine to eleven values were used to calculate the 'global' averages. Depending on the method used, a value represents either the mean of 120 individual analyses (for the *in situ* analytical methods) or the mean of 3–8 analyses (for the bulk analytical methods).

Ti, Mn, Cr, Co, Ni, Zn and Na: These seven elements show uniform distribution and good consistency between the mean values obtained by different microanalytical techniques and solution ICP-MS (Figure 3). The accepted data for Mn, Cr, Co, Ni and Zn agree within 1–3% (2 RSD – relative standard deviation), whereas the accepted data for Ti and Na agree within 6–8% (2 RSE; Table 8).

- Aluminium: The values obtained by solution ICP-MS in three different laboratories show large inter-laboratory variations, from 215 (± 24) μg g^{-1} to 310 (± 4) μg g^{-1}, while the values obtained by *in situ* techniques are more consistent. These variations in the mass fraction of Al obtained by solution ICP-MS can be explained by the presence of micro-inclusions (10–60 μm) of high-Al spinel [$(Mg_{0.8}, Fe_{0.2})(Cr_{0.18}, Al_{1.8})O_4$]. Only one such inclusion was observed at the surface of a polished olivine from more that 200 olivine fragments studied by SEM (Figure S1). This small spinel is colourless and is therefore almost impossible to detect optically inside olivine. Our data show that the presence of rare micro-inclusions of spinel containing 57–58% *w/w* of Al_2O_3 may be responsible for the increased aluminium content in the powders prepared for solution ICP-MS measurement. However, such

Table 8.
Suggested reference and information values for MongOL sh11-2

	Mass fraction	2*s*	2SE	2 RSE (%)	Method (*N***)
Major element oxides (% *m*/*m*)					
SiO_2	40.74	0.5	0.29	0.7	EPMA (2), XRF (1)
MgO	48.79	0.16	0.09	0.2	EPMA (2), Isotope dilution (1), XRF (1)
FeO	10.17	0.03	0.02	0.2	EPMA (2), Isotope dilution (1), XRF (1)
Minor and trace elements (μg g^{-1})					
Li	2.18	0.4	0.17	7.95	LA-ICP-MS (2), SIMS (1), sol ICP-MS (2)
Na	129.5	24	10	7.6	EPMA (1), LA-ICP-MS (2), sol ICP-MS (3)
Al	245	34	19	5.3	EPMA (2), LA-ICP-MS (3), SIMS (1), XRF (1)
P[a]	66.4	20	7	11	EPMA (1), XRF (1), LA-ICP-MS (4), sol ICP-MS (1)
Ca	688	59	34	5	EPMA (2), XRF (1)
Sc	3.4	0.2	0.11	3	LA-ICP-MS (4), SOL ICP-MS (3)
Ti	40.2	6	2	5.5	EPMA (1), LA-ICP-MS (3), SIMS (1), SOL ICP-MS (2)
V	5.5	0.5	0.24	4.3	LA-ICP-MS (3), SIMS (1), SOL ICP-MS (1)
Cr	125	9	3	2	EPMA (1), LA-ICP-MS (4), SIMS (1), SOL ICP-MS (4)
Mn	1119	47	15	1.3	EPMA (2), LA-ICP-MS (3), SIMS (1), SOL ICP-MS (3)
Co	148	12	4	2	EPMA (1), XRF (1), LA-ICP-MS (4), SIMS (1), SOL ICP-MS (3)
Ni	2822	87	29	1	EPMA (1), XRF (1), LA-ICP-MS (3), SIMS (1), SOL ICP-MS (3)
Cu	1.13	0.18	0.07	6.4	LA-ICP-MS (4), SIMS (1), SOL ICP-MS (1)
Zn	56.3	4.6	1.6	2.9	EPMA (1), XRF (1), LA-ICP-MS (4), SOL ICP-MS (2)
Ga [a]	0.1	0.02	0.01	13.7	LA-ICP-MS (3), SOL ICP-MS (1)
Sr [a]	0.007	0.0008	0.0004	6.2	LA-ICP-MS (4)
Y	0.079	0.014	0.005	6.9	LA-ICP-MS (3), SOL ICP-MS (3)
Zr [a]	0.044	0.009	0.005	11.2	LA-ICP-MS (4)
Dy [a]	0.006	0.0005	0.0003	4.2	LA-ICP-MS (3)
Ho [a]	0.003	0.001	0.0005	15.4	LA-ICP-MS (1), SOL ICP-MS (3)
Er	0.013	0.002	0.0007	5.3	LA-ICP-MS (3), SOL ICP-MS (4)
Tm	0.003	0.0004	0.0002	6.5	LA-ICP-MS (1), SOL ICP-MS (3)
Yb	0.029	0.002	0.0009	3.1	LA-ICP-MS (3), SOL ICP-MS (4)
Lu	0.007	0.0008	0.0003	5.1	LA-ICP-MS (1), SOL ICP-MS (4)

s, standard deviation; SE, standard deviation of the mean ('standard error'); RSE%, relative standard deviation of mean (in per cent); *N***, number of laboratories for each technique. [a] Information values.

an inclusion is easily visible in a polished olivine fragment in reflected light or under electron beam and thus can be easily avoided in microanalysis. The calculated value for Al is 245 ± 13 μg g^{-1}.

- Calcium: Contents of Ca show large discrepancies within LA-ICP-MS and solution ICP-MS data obtained in different laboratories (Figure 4). In contrast, EPMA data for Ca (Lab 1, Lab 6) obtained on different instruments using different matrix correction methods and different sets of primary reference materials are in excellent agreement and are also consistent with the XRF results (Figure 4). Given that ICP-MS-based methods have to use minor Ca isotopes that are subject to O^-, OH^- and N^- based

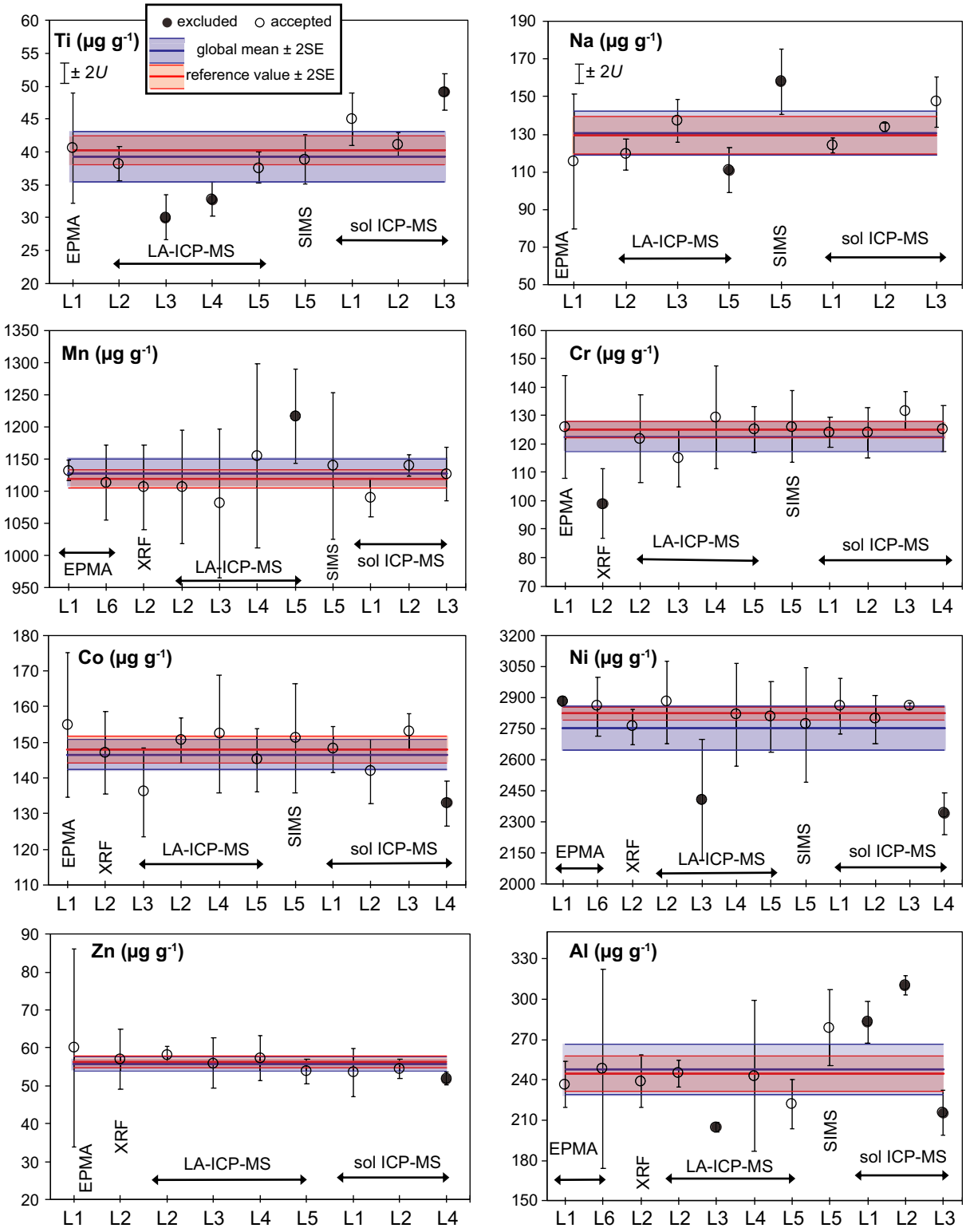

Figure 3. Mass fractions of Ti, Na, Mn, Cr, Co, Ni, Zn and Al obtained by different analytical techniques in different institutions. The thick blue horizontal lines show 'global' average of the means of the results of the labs in this study; blue horizontal field corresponds to two standard deviations of the mean (standard errors). The red thick horizontal lines represent the reference values derived in Table 8, and red field corresponds of two standard deviations of mean (standard error) of the reference value. The error bars for each value correspond to overall uncertainty of analytical method (2*U*) provided by each analytical laboratory.

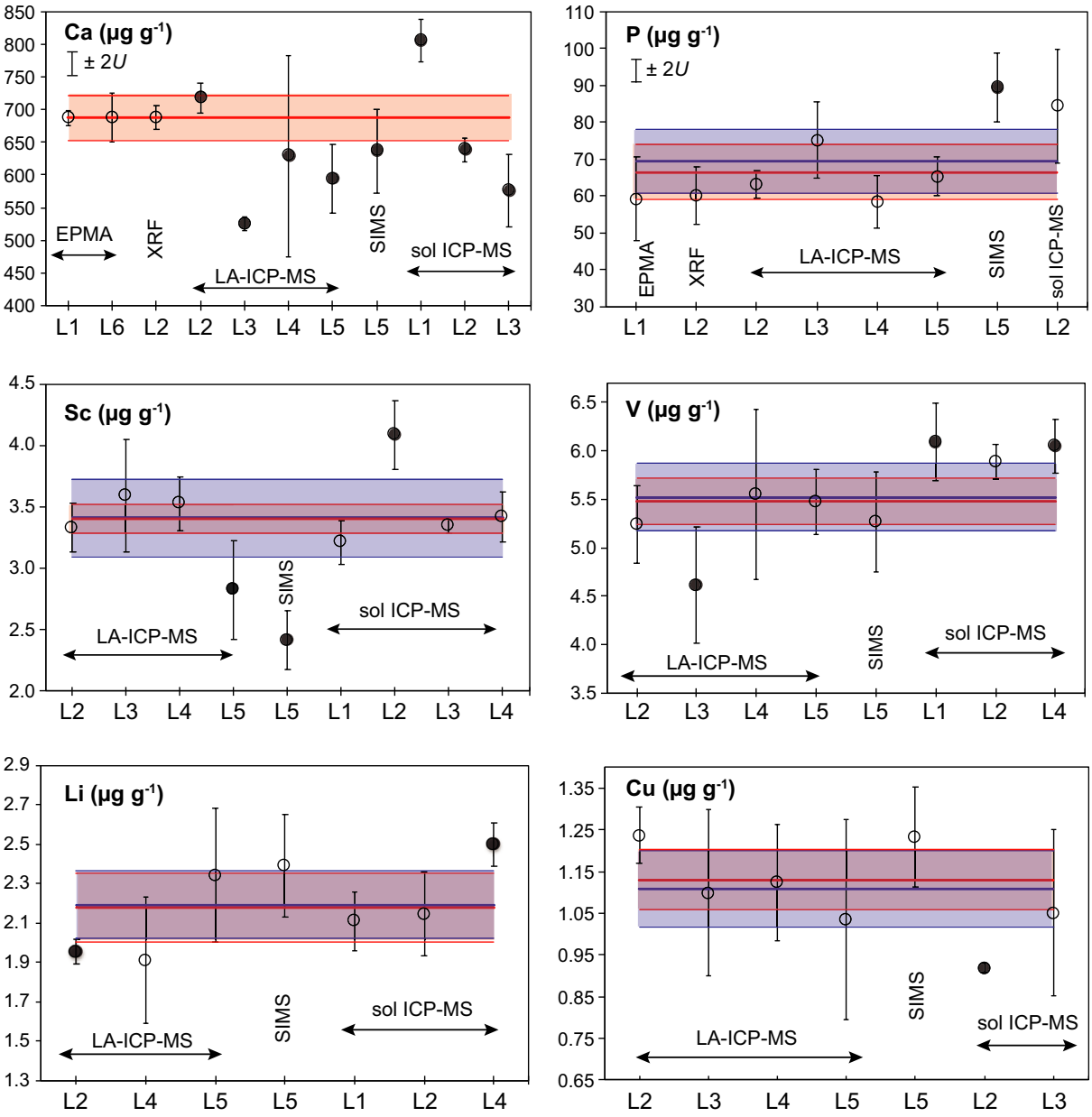

Figure 4. Mass fractions of Ca, P, Sc, V, Li and Cu obtained by different analytical techniques in different institutions. Symbols and horizontal lines as in Figure 3.

interferences from Mg and Si, we used EPMA and XRF data only to derive the reference value for Ca (Table 8), which fit almost all measurements within their errors (Figure 4). To be conservative we assign 5% (2 RSE) to this value.

- **Phosphorus:** This element is heterogeneously distributed between olivine fragments and shows the highest uncertainties of the mean values (12–29% 2 RSD of individual analysis; Table 6). Solution ICP-MS data were provided only by one laboratory and show values that are higher than reported by other techniques (Figure 3). The mean has 2 RSD of 11%, and we consider this as an information value.

Sc, V, Cu, Ga and Li

For this group of elements with mass fractions between 0.1 and 10 µg g^{-1}, LA-ICP-MS, SIMS (except Ga) and solution ICP-MS data are available (Table 6, Figures 4 and 5). In general, data for Sc, V, Li and Ga are consistent between different laboratories and methods; however, in each case one or two outliers were observed (Figures 4 and 5).

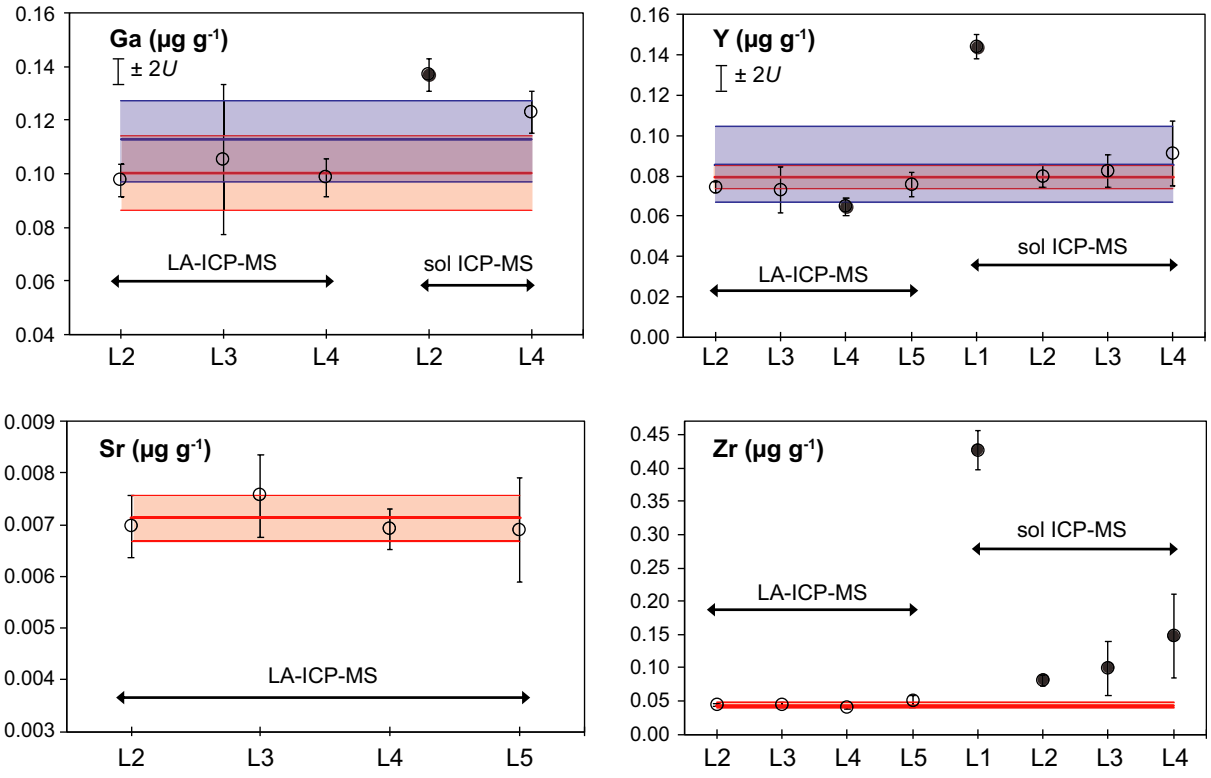

Figure 5. Mass fractions of Ga, Y, Sr, and Zr obtained by different analytical techniques in different institutions. Symbols and horizontal lines as in Figure 3.

Yttrium

Four data sets of both LA-ICP-MS and solution ICP-MS analyses are available (Figure 5) and, with the exception of two outliers, show an overall mean of 0.079 (± 0.005) µg g^{-1} (Table 8).

Strontium and zirconium

Solution ICP-MS data shows strong variation between laboratories and values are up to several orders of magnitude greater than LA-ICP-MS. This suggests that some sort of contamination occurred with the solution analyses. Some of this could be due to acid blanks or 'carryover' effects; however, we believe that the most likely explanation is the possible presence of secondary melt/fluid micro-inclusions in olivine, which contain these incompatible elements. The mean of four LA-ICP-MS data sets for Zr is 0.044 (± 0.005) µg g^{-1} and for Sr is 0.007 (± 0.0004) µg g^{-1}.

Dy, Ho, Er, Tm, Yb, Lu

The mass fractions of these high atomic number REE are given in Table 7. For dysprosium, the solution ICP-MS data were excluded from consideration for the same reason as for Sr and Zr (see discussion above). For other HREE, the data sets of solution ICP-MS and LA-ICP-MS are in good agreement with each other.

The accepted composition of olivine MongOL Sh11-2 (major, minor and trace elements) passes both criteria of analytical quality, i.e., stoichiometry (3.002 cations per four oxygen) and analytical total (100.40% *w/w*; Table 9).

Conclusions

The fragments of natural olivine separated from the inner part of a xenolith of mantle spinel lherzolite (MongOL Sh11-2) are sufficiently homogeneous to be used as a matrix-matched reference material for *in situ* microanalysis of olivine by EPMA, LA-ICP-MS and SIMS. Some 120 olivine fragments were studied, involving > 1020 *in situ* analyses by EPMA, LA-ICP-MS and SIMS. In addition, eight aliquots were analysed by ID-ICP-MS, nine aliquots were analysed by solution ICP-MS, and two aliquots by XRF. Analyses were performed in six different analytical laboratories. Well-characterised reference values were obtained for major elements (Si, Mg, Fe), minor elements (Ni, Mn) and trace elements (Li, Na, Al, Ca, Sc, Ti, V, Cr, Co, Cu, Zn, Y, Er, Tm, Yb and Lu).

Table 9.
Stoichiometry for MongOL Sh11-2

Oxide (% *m/m*)	MongOL Sh11-2	2*s*
Na_2O	0.0174	0.0013
Al_2O_3	0.0462	0.0025
CoO	0.0188	0.0005
ZnO	0.0070	0.0002
P_2O_5	0.0152	0.0017
CaO	0.0962	0.0048
TiO_2	0.0067	0.0004
NiO	0.3591	0.0037
MnO	0.1445	0.0019
Cr_2O_3	0.0182	0.0004
MgO	48.79	0.09
FeO	10.17	0.02
SiO_2	40.74	0.29
Total oxide	100.43	
Cations (formula unit)		
Na	0.0008	
Al	0.0013	
Co	0.0004	
Zn	0.0001	
P	0.0003	
Ca	0.0025	
Ti	0.0001	
Ni	0.0071	
Mn	0.0030	
Cr	0.0004	
Mg	1.7803	
Fe^{2+}	0.2082	
Si	0.9972	
Total cations	3.0017	
Oxygen	4.0000	

Fo = 100*Mg/(Mg + Fe^{2+}) = 89.53.

Significant heterogeneity was detected for mass fraction of phosphorus (heterogeneity index 12.4). Minor heterogeneity (heterogeneity index of 1–2) was also detected for contents of Li, Na, Al, Sc, Ti and Cr.

The data obtained for Ga, Sr, Zr, Dy and Ho are considered information values because these elements show significant inconsistency between mass fractions obtained by LA-ICP-MS and solution ICP-MS. We interpret this as an indication of the possible presence of melt/fluid micro-inclusions in olivine, which affect solution ICP-MS data.

Olivine reference material MongOL Sh11-2 is available upon request (valentina.batanova@univ-grenoble-alpes.fr) as sets of 10–15 olivine fragments (fraction 1–2 mm).

Acknowledgements

VB thanks V. Magnin for assistance in maintenance the EPMA Facility in ISTerre and R.W. Carlson for providing the xenoliths. MP and DGS are grateful to Ulrike Westernströer for assistance with ICP-MS at CAU. The authors thank Paul Sylvester for editorial handling and review and one anonymous reviewer for comprehensive and constructive comments that helped to improve and clarify the article. This study was supported by BQR ISTerre grant (VB), the Russian Science Foundation 14-17-00491 and R. Lounsbery foundation grants (AVS), maintenance of EPMA facility at ISTerre was partly supported by Labex OSUG@2020 (Investissements d'avenir–ANR10 LABX56) and Institut Universitaire de France (IUF). Analyses at JAMSTEC were partially supported by the JSPS KAKENHI grants JP7162441, JP15H02148, JP16H01125 and JP18H04372 to J.-I.K.

References

Application Note 1 (2010)
Comparison of a measurement result with the certified value. European Commission – Joint Research Centre Institute for Reference Materials and Measurement (Geel), 2pp.

Batanova V.G., Sobolev A.V. and Kuzmin D.V. (2015)
Trace element analysis of olivine: High precision analytical method for JEOL JXA-8230 electron probe microanalyser. Chemical Geology, 419, 149–157.

Batanova V.G., Sobolev A.V. and Magnin V. (2018)
Trace element analysis by EPMA in geosciences: Detection limit, precision and accuracy. Emas 2017 Workshop – 15th European Workshop on Modern Developments and Applications in Microbeam Analysis and Iumas-7 Meeting – 7th Meeting of the International Union of Microbeam Analysis Societies, 304. IOP Publishing Ltd (Bristol, UK).

Boyd F.R., Finger L.W. and Chayes F. (1967)
Computer reduction of electron-probe data. Carnegie Institution of Washington Yearbook, 67, 21–215.

Carlson R.W. and Ionov D.A. (2019)
Compositional characteristics of the MORB mantle and Bulk Silicate Earth based on spinel peridotites from the Tariat Mongolia. Geochimica et Cosmochimica Acta, in press, GCA-D-19-00197

Chang Q., Shibata T., Shinotsuka K., Yoshikawa M. and Tatsumi Y. (2003)
Precise determination of trace elements in geological standard rocks using inductively coupled plasma-mass spectrometry. Frontier Research on Earth Evolution, 1, 357–362.

Chauvel C., Bureau S. and Poggi C. (2011)
Comprehensive chemical and isotopic analyses of basalt and sediment reference materials. Geostandards and Geoanalytical Research, 35, 125–143.

references

Coogan L.A., Saunders A.D. and Wilson R.N. (2014)
Aluminium-in-olivine thermometry of primitive basalts: Evidence of an anomalously hot mantle source for large igneous provinces. Chemical Geology, 368, 1–10.

De Hoog J.C.M., Gall L. and Cornell D.H. (2010)
Trace-element geochemistry of mantle olivine and application to mantle petrogenesis and geothermobarometry. Chemical Geology, 270, 196–215.

Garbe-Schönberg D. (1993)
Simultaneous determination of thirty-seven trace elements in twenty-eight international rock standards by ICP-MS. Geostandards Newsletter, 17, 81–97.

Gilbert S., Danyushevsky L., Robinson P., Wohlgemuth-Ueberwasser C., Pearson N., Savard D., Norman M. and Hanley J. (2013)
A comparative study of five reference materials and the Lombard meteorite for the determination of the platinum-group elements and gold by LA-ICP-MS. Geostandards and Geoanalytical Research, 37, 51–64.

GUM (2008)
Evaluation of measurement data – Guide to the expression of uncertainty in measurement. Joint Committee for Guides in Metrology, JCGM 100:2008.

Harries D. (2014)
Homogeneity testing of microanalytical reference materials by electron probe microanalysis (EPMA). Chemie der Erde —Geochemistry, 74, 375–384.

Ionov D.A. (2007)
Compositional variations and heterogeneity in fertile lithospheric mantle: Peridotite xenoliths in basalts from Tariat, Mongolia. Contributions to Mineralogy and Petrology, 154, 455–477.

Ionov D.A. and Hofmann A.W. (2007)
Depth of formation of subcontinental off-craton peridotites. Earth and Planetary Science Letters, 261, 620–634.

ISO Guide 35 (2017)
Reference materials – Guidance for characterization and assessment of homogeneity and stability. International Organization for Standardization (Geneva), 106pp.

Jarosewich E.J., Nelen J.A. and Norberg J.A. (1980)
Reference samples for electron microprobe analysis. Geostandards Newsletter, 4, 43–47.

Jochum K.P., Dingwell D.B., Rocholl A., Stoll B., Hofmann A.W., Becker S., Besmehn A., Bessette D., Dietze H.J., Dulski P., Erzinger J., Hellebrand E., Hoppe P., Horn I., Janssens K., Jenner G.A., Klein M., McDonough W.F., Maetz M., Mezger K., Münker C., Nikogosian I.K., Pickhardt C., Raczek I., Rhede D., Seufert H.M., Simakin S.G., Sobolev A.V., Spettel B., Straub S., Vincze L., Wallianos A., Weckwerth G., Weyer S., Wolf D. and Zimmer M. (2000)
The preparation and preliminary characterisation of eight geological MPI-DING reference glasses for *in-situ* microanalysis. Geostandards Newsletter: The Journal of Geostandards and Geoanalysis, 24, 87–133.

Jochum K.P., Nohl L., Herwig K., Lammel E., Stoll B. and Hofmann A.W. (2005)
GeoReM: A new geochemical database for reference materials and isotopic standards. Geostandards and Geoanalytical Research, 29, 333–338.

Jochum K.P., Stoll B., Herwig K., Willbold M., Hofmann A.W., Amini M., Aarburg S., Abouchami W., Hellebrand E., Mocek B., Raczek I., Stracke A., Alard O., Bouman C., Becker S., Ducking M., Bratz H., Klemd R., de Bruin D., Canil D., Cornell D., de Hoog C.J., Dalpe C., Danyushevsky L., Eisenhauer A., Gao Y.J., Snow J.E., Goschopf N., Gunther D., Latkoczy C., Guillong M., Hauri E.H., Hofer H.E., Lahaye Y., Horz K., Jacob D.E., Kassemann S.A., Kent A.J.R., Ludwig T., Zack T., Mason P.R.D., Meixner A., Rosner M., Misawa K.J., Nash B.P., Pfander J., Premo W.R., Sun W.D., Tiepolo M., Vannucci R., Vennemann T., Wayne D. and Woodhead J.D. (2006)
MPI-DING reference glasses for *in situ* microanalysis: New reference values for element concentrations and isotope ratios. Geochemistry, Geophysics, Geosystems, 7, 1–44.

Jochum K.P., Weis U., Schwager B., Stoll B., Wilson S.A., Haug G.H., Andreae M.O. and Enzweiler J. (2016)
Reference values following ISO guidelines for frequently requested rock reference materials. Geostandards and Geoanalytical Research, 40, 333–350.

Kimura J.-I. and Chang Q. (2012)
Origin of suppressed matrix effect for improved analytical performance in determination of major and trace elements in anhydrous silicate samples using 200-nm femtosecond laser ablation sector field-inductively coupled plasma-mass spectrometry. Journal of Analytical Atomic Spectrometry, 27, 1549–1559.

Longerich H.P., Jackson S.E. and Günther D. (1996)
Laser ablation inductively coupled plasma-mass spectrometric transient signal data acquisition and analyte concentration calculation. Journal of Analytical Atomic Spectrometry, 11, 899–904.

Makishima A. and Nakamura E. (2006)
Determination of major, minor and trace elements in silicate samples by ICP-QMS and ICP-SFMS applying isotope dilution-internal standardisation (ID-IS) and multi-stage internal standardisation. Geostandards and Geoanalytical Research, 30, 245–271.

Makishima A., Nakamura E. and Nakano T. (1999)
Determination of zirconium, niobium, hafnium and tantalum at ng g^{-1} levels in geological materials by direct nebulisation of sample HF solution into FI-ICP-MS. Geostandards Newsletter: The Journal of Geostandards and Geoanalysis, 23, 7–20.

Makishima A., Kobayashi K. and Nakamura E. (2002)
Determination of chromium, nickel, copper and zinc in milligram samples of geological materials using isotope dilution high resolution inductively coupled plasma-mass spectrometry. Geostandards Newsletter: The Journal of Geostandards and Geoanalysis, 26, 41–51.

Mallmann G. and O'Neill H.S. (2013)
Calibration of an empirical thermometer and oxybarometer based on the partitioning of Sc, Y and V between olivine and silicate melt. Journal of Petrology, 54, 933–949.

references

Müller W., Shelley M., Miller P. and Broude S. (2009)
Initial performance metrics of a new custom-designed ArF excimer LA-ICP-MS system coupled to a two-volume laser-ablation cell. **Journal of Analytical Atomic Spectrometry**, **24**, 209–214.

Nakamura K. and Chang Q. (2007)
Precise determination of ultra-low (sub-ng g^{-1}) level rare earth elements in ultramafic rocks by quadrupole ICP-MS. **Geostandards and Geoanalytical Research**, **31**, 185–197.

Norman M., Robinson P. and Clark D. (2003)
Major- and trace-element analysis of sulfide ores by laser-ablation ICP-MS, solution ICP-MS, and XRF: New data on international reference materials. **Canadian Mineralogist**, **41**, 293–305.

Pankhurst M.J., Walshaw R. and Morgan D.J. (2017)
Major element chemical heterogeneity in Geo2 olivine microbeam reference material: A spatial approach to quantifying heterogeneity in primary reference materials. **Geostandards and Geoanalytical Research**, **41**, 85–91.

Potts P.J. (2012)
Glossary of analytical and metrological terms from the International Vocabulary of Metrology (2008). **Geostandards and Geoanalytical Research**, **36**, 231–246.

Potts P.J., Tindle A.G. and Isaacs M.C. (1983)
On the precision of electron-microprobe data – A new test for the homogeneity of mineral standards. **American Mineralogist**, **68**, 1237–1242.

Press S., Witt G., Seck H.A., Ionov D. and Kovalenko V.I. (1986)
Spinel peridotite xenoliths from the Tariat depression, Mongolia. I: Major element chemistry and mineralogy of a primitive mantle xenolith suite. **Geochimica et Cosmochimica Acta**, **50**, 2587–2599.

Robinson P., Townsend A.T., Yu Z. and Münker C. (1999)
Determination of scandium, yttrium and rare earth elements in rocks by high resolution inductively coupled plasma-mass spectrometry. **Geostandards Newsletter: The Journal of Geostandards and Geoanalysis**, **23**, 31–46.

Shimizu N. and Hart S.R. (1982)
Applications of the ion microprobe to geochemistry and cosmochemistry. **Annual Review of Earth and Planetary Sciences**, **10**, 483–526.

Sobolev A.V., Hofmann A.W., Sobolev S.V. and Nikogosian I.K. (2005)
An olivine-free mantle source of Hawaiian shield basalts. **Nature**, **434**, 590–597.

Sobolev A.V., Hofmann A.W., Kuzmin D.V., Yaxley G.M., Arndt N.T., Chung S.L., Danyushevsky L.V., Elliott T., Frey F.A., Garcia M.O., Gurenko A.A., Kamenetsky V.S., Kerr A.C., Krivolutskaya N.A., Matvienkov V.V., Nikogosian I.K., Rocholl A., Sigurdsson I.A., Sushchevskaya N.M. and Teklay M. (2007)
The amount of recycled crust in sources of mantle-derived melts. **Science**, **316**, 412–417.

Sylvester P. (2008)
Matrix effects in laser ablation ICP-MS. **In: Sylvester P. (ed.), Laser ablation ICP-MS in the Earth sciences: Current practices and outstanding issues. Mineralogical Association of Canada, Short Course Series**, **40**, 67–78.

Wan Z.H., Coogan L.A. and Canil D. (2008)
Experimental calibration of aluminum partitioning between olivine and spinel as a geothermometer. **American Mineralogist**, **93**, 1142–1147.

Yu Z., Robinson P., Townsend A.T., Münker C. and Crawford A.J. (2000)
Determination of HFSE, Rb, Sr, Mo, Sb, Cs, Tl and Bi at ng g^{-1} levels in geological reference materials by magnetic sector ICP-MS after HF/$HClO_4$ high pressure digestion. **Geostandards Newsletter: The Journal of Geostandards and Geoanalysis**, **24**, 39–50.

Supporting information

The following supporting information may be found in the online version of this article:

Figure S1. SEM photograph of a spinel inclusion at the surface of a polished olivine fragment.

Table S1. Geochemical composition of three independent dissolutions of olivine reference material MongOL Sh11-2 by ICP-MS.

Table S2. *F*-test results for reference material MongOL Sh11-2.

This material is available from: http://onlinelibrary.wiley.com/doi/10.1111/ggr.12266/abstract (This link will take you to the article abstract).